EEET ECOLOGICAL ENGINEERING & ENVIRONMENTAL TECHNOLOGY

Ecological Engineering & Environmental Technology 2024, 25(11), 308–320
https://doi.org/10.12912/27197050/192775
ISSN 2299–8993, License CC-BY 4.0

Received: 2024.08.13
Accepted: 2024.09.15
Published: 2024.10.01

Development of Nanocellulose Hydrogels from Sargassum Seaweed as Controlled Nutrient Release Systems and their Application in Germination

Jeycob Rodríguez-Quesada[1], Karina Rodríguez Mora[2,3*], César A. Bernal-Samaniego[1], Eddy G. Jirón-García[1], Carlos Rojas-Alvarado[2,4]

[1] Universidad de Costa Rica, Sede del Caribe, Limón, Costa Rica
[2] Unidad de Recursos Forestales, Instituto de Investigaciones en Ingeniería, Universidad de Costa Rica, San José, Costa Rica
[3] Centro de Investigación Ciencia e Ingeniería de Materiales, Universidad de Costa Rica, San José, Costa Rica
[4] Escuela de Ingeniería de Biosistemas, Universidad de Costa Rica, San José, Costa Rica
* Corresponding author's e-mail: karina.rodriguezmora@ucr.ac.cr

ABSTRACT

Sargassum algae, being able to proliferate without the need to be attached to a substrate, travel through the ocean generating massive stagnations on the Caribbean coasts of the continent, becoming an environmental problem. Because its composition mainly includes polysaccharides, such as cellulose and hemicellulose, these algae were used to produce nanocellulose and create hydrogels to apply to germination. This article aims to develop of nanocellulose hydrogels from Sargassum and study the effect of it adding nanocellulose hydrogels from Sargassum algae loaded with Ca-PO_4- and NO_3 as nutrients in the germination process. The Sargassum algae used underwent two hydrolysis processes, one basic and one acid, with which it was possible to increase the cellulose content from 25.7 ± 0.42% to 34.05 ± 0.39 after the first hydrolysis and after 90.15 ± 0.44% after the second. Size reduction to nanocellulose was performed employing an ultrasonic homogenizer sonicator. The obtained nanocellulose was characterized using infrared spectroscopy, X-ray diffraction, and transmission electron microscopy, showing that by the alkaline method, the sizes were between 135–190 nm while by the acid method, the fiber sizes were between 108–163 nm with a difference of 1.04 in the crystallinity index between the two hydrolyses. With the nanocellulose, hydrogels were formed using 5%, 10%, and 15% borax as crosslinking agents. Drying curves and scanning electron microscopy were performed on the hydrogels. Nutrients Ca-PO_4-NO_3 were added to the hydrogel and their release in water was studied through Ultraviolet-Visible spectrophotometry, with which it was decided to use the hydrogel containing 10% borax in the germination study. The effect of the hydrogel loaded with nutrients on the germination of bean and linseed seeds employing a complete factorial design 23. Obtaining results that the nutrient with the greatest influence on germination was nitrogen while the nutrient with the least favorable results was the match.

Keywords: agriculture, biomass, nanomaterials.

INTRODUCTION

Marine algae are a type of algae that grows in coastal areas or shallow waters at the edge of the ocean, traditionally classified as green algae, red algae, and brown algae (Nagappan et al., 2017). *Sargassum* algae belong to the brown algae and have the particularity that they live floating without the need to remain attached to a substrate, unlike other species (Franks et al., 2016), due to this quality, they can be found free in the sea ocean and travel long distances across it.

These characteristics have caused *Sargassum* algae to form what is known as the Sargasso Sea in the central part of the Atlantic Ocean (Wang et al., 2019), however, since 2011, massive

stagnation events have occurred sargassum off the coasts of Caribbean islands and Mexico (Lu et al., 2019), although similar events have also been reported in West Africa, northern Brazil (Gower and King, 2019), and recently in Central America (Chopped, 2022). Associating the growth of this algae with the effects of climate change, marine currents, and excess nutrients in the sea (Maurer et al., 2015; Wang et al., 2018).

This excessive growth in *Sargassum* algae causes health, environmental and economic problems due to the demand for the oxygen they require, which causes the death of fish and shrimp, while their decomposition generates gases such as CO_2, methane, and ammonia and generates sulfites that acidify the waters and affect coral reefs, without taking into account the proliferation of small crustaceans in the algae that have washed up on the coasts, the bad appearance and bad smell (Gower and King, 2019; Lu et al., 2019; Maurer et al., 2015; Resiere et al., 2018).

As a consequence of this, the presence in various latitudes of *Sargassum* brown algae has aroused the interest of different research centers, due to its multiple applications in sectors such as agri-food, cosmetics, textiles, and pharmaceuticals (Mattio and Payril, 2011; Nagappan et al., 2017) since they contain carotenoids, fiber, in addition to having polysaccharides including alginate and cellulose (Yende et al., 2014), the latter can be used in various fields such as the formation of hydrogels in its form nanocellulose.

A hydrogel is a three-dimensional network-like conformation of a polymer that is capable of retaining several times its dry weight of water or biological fluids (Supramaniam et al., 2018), nanocellulose on the other hand, is the nanometric form of cellulose that can It can be obtained mainly in three ways: (1) nanocrystalline cellulose and cellulose nanocylinders (2) cellulose nanofibrils and (3) bacterial cellulose, depending on the method of obtaining it, the final application and the desired physical and chemical characteristics (Jirón García et al., 2020, 2022).

Due to their properties, hydrogels have been used in the agricultural field and environmental protection at the time of sowing, applied as auxiliaries in the management of the plantation, and to protect the roots using as its main characteristic the high capacity of retention of water (Fernández and Gallo, 2018). However, the application of hydrogels in agriculture is not limited to a water supply in arid soils. Controlled release formulations for pesticides and nutrients have become attractive because the degradation of the active agent can be mitigated and its effect prolonged, as well as lessen the negative impact of fertilizing agents on the soil (Liu et al., 2021; Rudzinski et al., 2002; Wang et al., 2021).

This article aims to develop of nanocellulose hydrogels from Sargassum and study the effect of it adding nutrient-loaded nanocellulose hydrogels from *Sargassum* algae on seed germination because recently, several investigations have indicated that hydrogels could act as seed culture media by conserving water and nutrients that help in germination, for example, Ramírez et al. (2007) demonstrated that using absorbent gels in tomato seeds, accelerated the germination process by 78% and reduced the amount of non-germinated sources for the same seeds type, but without using hydrogels, Zhang et al. (2017), carried out seed germination experiments where they confirmed that anionic cellulose hydrogels with adequate carboxylate contents could act as plant growth regulators and promote germination and seed growth, Akhter et al. (2004), showed that hydrogels do not influence the germination of barley and wheat in sandy soils but they do influence that of chickpeas, as well as Pazderů and Koudela, (2013) showed that in Hydrogels with low water content do not influence the germination of lettuce and onion as do hydrogels with abundant liquid.

METHODOLOGY

Biomass collection and obtaining nanocellulose

Specimens of the *Sargassum polyceratium* Montagne algae were collected in the town of Cocles in the southern sector of the Limón coast. The collected material was pretreated according to Mesén et al. (2023) with modification, for that biomass was dried in an oven at a temperature of 70 °C for 24 hours. Once dry; the size of the biomass was reduced using a blade mill until reaching a sample size of 50 mm. Subsequently, a second reduction was made using a cutting mill, so that the samples had a size of 60 μm. Finally, said the sample was sieved using a 5 μm sieve to guarantee the desired size.

Basic hydrolysis was performed, and 2 grams of biomass were placed in Erlenmeyers, to which 50 mL of 2% sodium hydroxide was added. The

samples were placed inside the autoclave to be processed at 1.2 bar and 121 °C for 30 minutes. The biomass obtained was washed with water until a neutral pH was obtained. Subsequently, the cellulose was left to rest for 30 minutes with 50 mL of sodium hypochlorite to bleach the fibers, after which the samples were filtered and washed until excess chlorine was eliminated. Next, an acid hydrolysis process was used with the same previous conditions, but using 6% acetic acid. The cellulose obtained was washed with water until a neutral pH was obtained. To carry out the mechanical rupture, the Qsonica Model Q700 sonicator was used, and the sample was placed in a cold-water bath for 30 minutes with 60% amplitude (Jirón et al., 2020).

Characterization

The determination of the composition was made based on the TAPPI standard: T280 pm-99 (TAPPI, 1999), as well as on the technical reports: NREL/TP-510-42620 (Hames et al., 2008), NREL/TP -510-42618 (Sluiter et al., 2012).

To obtain the bands of the functional groups associated with the fiber components, as well as the absence and presence of lignin, a PerkinElmer Frontier FT-IR-ATR model was used 16 scans per sample were made. The scan was from 4000 cm^{-1} to 450 cm^{-1}. The Bruker D8 Advance diffraction equipment with LynxEye detector was used to determine the degree of crystallinity of the cellulose present in the fibers obtained, before and after each hydrolysis step. The fiber sizes of the obtained nanocellulose were determined using a HITACHI HT 7700 transmission electron microscope. For this, nanocellulose solutions with a concentration of 1 mg/L were prepared and placed on carbon grids (Kljun et al., 2011).

Nanocellulose hydrogels with sodium tetraborate (borax) were developed to increase the consistency of the biopolymer, therefore, the use of 5%, 10%, and 15% borax was studied. Both compounds were mixed for 30 minutes. Subsequently, the sample was centrifuged for 10 minutes at 100 rpm in a CENCE model TDZ4 centrifuge. To carry out this process, a Radwag brand MA-50. R moisture balance was used. After this, the mass obtained was measured for 90 minutes at 5-minute intervals (Liu et al., 2020).

A HITACHI model S700-N scanning electron microscope was used to determine morphological changes in the hydrogel. To observe its porosity in a high vacuum, a drying process of the hydrogel was carried out and it was re-hydrated with the inclusion of paraffin. Once the moisture percentages of each hydrogel were determined, this information was used to add the different solid nutrients so that the existing water in the sample dissolved them, each one with a concentration of 100 mg/L. In this way, it was guaranteed that the solid was trapped inside the hydrogel for a release process by osmosis (Svobodová et al., 2012).

Water nutrient release curves and germination tests

To know the release of each nutrient in the different types of hydrogels, 5 grams of hydrogel were placed in 500 mL of water. Subsequently, an aliquot of water was collected for each time studied. This process was carried out for the three selected nutrients (potassium dihydrogen phosphate, potassium nitrate, and calcium carbonate) and the hydrogels with different amounts of borax (5%, 10%, and 15%). The concentration values obtained were plotted against the collection times to obtain said curves.

A complete factorial design 2^3 was used, in which the germination percentage (number of germinated seeds) and plant growth (stem size) were established as effects. For this, two types of seeds were used (generalist and specialist). In this case, beans were used as a generalist seed and flaxseed was used as a specialist seed. The analysis factor was fertilization and within these three levels corresponding to each of the evaluated nutrients were studied. Thus, the 2^3-shaped design with 5 replicates evaluated the effect of each nutrient and the effect of nutrient combinations on the response variables.

A 200-space plastic germination tray was used. In each space of the germination tray, a first layer of soil equivalent to 45 mL was placed. Then, a second layer made up of 1 mL of hydrogel was added and finally, a last layer of soil of 30 mL was placed. The corresponding seeds were deposited on the latter. A syringe was used to dose 5 mL of water to each seed every day to guarantee irrigation uniformity. To record germination, the seeds were checked on day 5 and day 12 after sowing. On day 5 after sowing, the tests were reviewed to document the seed germination process. On day 12 each seed was taken; its germination was verified, and the length of the germinated radicle was measured with the use of a vernier (Zhang et al., 2017).

RESULTS AND DISCUSSION

The composition of the algae analyzed is shown in Table 1, as can be seen, *Sargassum* algae have a percentage of holocellulose (cellulose + hemicellulose) equivalent to 78.84% by weight of the total biomass, a percentage that is considered high in comparison with other studies carried out on algae of the same type where hemicellulose contents of 19.6 ± 0.9% are reported (Tamayo and Del Rosario, 2014), in addition to showing values higher than those reported for different types of brown algae, in where it is mainly pointed out that the algae have a low lignin content and cellulose content ranging from 43.00 ± 2.11 % to 74.00 ± 3.45 % (Salem and Ismail, 2022) and due to its similarity with the value reported for ceiba (79.08%) (Honorato-Salazar et al., 2016). These natural variations depend on the oceanic sector from which said algae come (Van Tussenbroek, 2016), and on the climatic season in which they are collected as a direct consequence of the photosynthetic process carried out (Marinho-Soriano et al., 2006).

After carrying out the basic hydrolysis with NaOH, it can be noted how the percentages of lignin, ashes, and extractives decreased, this is a consequence of the fact that this base helps to solubilize and extract the lignin from the biomass by affecting the acetyl group in the hemicellulose and the lignin ester-carbohydrate linkages (Hassan and Badri, 2014). Even though alkaline hydrolysis presents a low energy and reagent cost to obtain cellulose, additional acid hydrolysis with acetic acid is used to facilitate the reduction of the size of cellulose microfibers on a nanometric scale (García and Mora, 2022). The isolation of cellulose nanocrystals has been reported following a series of steps ranging from alkaline hydrolysis, and bleaching to acid hydrolysis with strong acids (Chávez-Guerrero et al., 2022), however, nanofibers can be obtained using a similar series of steps, but with a weak acid such as acetic acid (Mesén and Mora, 2021).

Once the acid hydrolysis was carried out, the hemicellulose decreased and the cellulose content increased, because hemicellulose is associated with the non-crystalline regions of the material (Patel and Parsania, 2018). The amorphous zones of the fibers were reduced in cellulosic fibers, this is important since it has been shown that high values of holocellulose in the amorphous phase make it difficult to mechanically reduce the size of nanocellulose (García et al., 2020).

Finally, the mass percentages reported in the literature vary from species to species, however, for the Sargassum alga, they can reach up to 22.00% (Ai et al., 2022; Jones and Mayfield, 2012) so the analysis shown below these averages. Such values are considered even lower when compared with more rigid biomass such as coconut fiber, 45–50%, and (Deepa et al., 2015) banana rachis 17.3% (Alzate-Arbeláez et al., 2019) or pineapple stubble 20% (Sun et al., 2000). Due to the above, brown algae have been proposed to have an advantage over terrestrial biomass due to the little lignin or lignin-like compounds they present (Schiener et al., 2015).

In the infrared spectra, different bands can be noted. A strong and broadband can be observed between 3450 cm^{-1} and 3200 cm^{-1} associated with stretching vibration of the O-H hydrogen bond present in cellulose and hemicellulose (Schwanninger et al., 2004). The presence of a 3420 cm^{-1} signal was also identified, which is due to the stretching of the C-H groups and one at 2910 cm^{-1} due to the C-H stretching (Sun et al., 2004).

In addition, a characteristic signal is noted as a result of vibrations due to the stretching of the C = O bond that the hemicellulose possesses (1760–1630 cm^{-1}) (Pavia et al., 2009). It can be seen that the algae sample after basic hydrolysis has a higher signal intensity than the other samples, which supports the values obtained

Table 1. Characterization results for each of the fibers

Substance	Algae		Basic hydrolysis		Acid hydrolysis	
	Average (%)	Deviation (±)	Average (%)	Deviation (±)	Average (%)	Deviation (±)
Fat-soluble extractives	2.46	0.09	0.0090	0.0002	0.00866	0.00017
Cellulose	25.70	0.42	34.05	0.39	90.15	0.44
Hemicellulose	53.14	0.28	63.72	0.29	8.31	0.21
Lignin	11.19	0.04	0.11	0.02	0.099	0.009
Ashes	1.23	0.10	0.044	0.003	0.033	0.002

in Table 2 since this sample is the one with the highest concentration of such a compound. In addition, in the region that goes from 1600 cm^{-1} to 1475 cm^{-1}, it is typical to find the characteristic bands that show the presence of C = C groups corresponding to the aromatic rings of lignin. This signal has a characteristic shape in the established range (Pavia et al., 2009); as can be seen in the Figure 1. This set of signals is diminished or eliminated after alkaline and acid treatment, which is why it can be considered as another way of evidencing lignin removal after each procedure.

Finally, between 1066 cm^{-1} and 1050 cm^{-1}, an elongated and narrow peak is noted in the infrared spectrum, characteristic of the C-O-C groups of the rings with a β-glucosidic bond (García et al., 2022).

In Figure 1, using the lines that mark the exact wavelength value for each of the groups of interest, it can be seen how there is a reduction in the intensity of signals that refer to lignin. This suggests the removal of the said compound during the hydrolysis processes. In the case of the signal detected at 1022.37 cm^{-1}, typical of cellulose, it can be noted that the algae sample after basic and acid hydrolysis presents the highest intensity at said wavelength, which suggests that the fibers after acid hydrolysis have a higher percentage of said biopolymer (Hospodarova et al., 2018).

The cellulose present in the fibers changed its crystallinity after going through the hydrolysis processes, according to the Crystallinity Index. To determine this index, the cellulose is used after each hydrolysis, and Equation 1 is used (Segal et al., 1959):

$$CrI = \frac{I_{002} - I_{am}}{I_{200}} \times 100 \quad (1)$$

In the said equation, the value of I_{002} is defined as the degrees at which the highest intensity peak is detected while I_{am} represents the degrees at which the lowest intensity peak value is located. After the calculations, the results can be seen in Table 3. When observing the IC values presented, an increase in the crystallinity of the fibers is noted

Table 2. Characteristic wavelengths of lignocellulosic materials

Theoretical wavelength (cm^{-1})	Wavelength obtained (cm^{-1})	Signal description	Reference
3450–3200	3278.56	O-H groups present in cellulose/ hemicellulose	(Schwanninger et al., 2004)
3000–2850	2917.24	C-H groups present in cellulose	(Ray and Sain, 2017)
1760–1600	1605.41	C=O groups present in hemicellulose	(Sills and Gossett, 2012)
1600–1400	1418.59	C=C bonds of the aromatic rings of lignin	(Kubo and Kadla, 2005)
1066–1010	1022.37	C-O-C groups are present in the β-glucosidic ring of cellulose	(Kubo and Kadla, 2005)

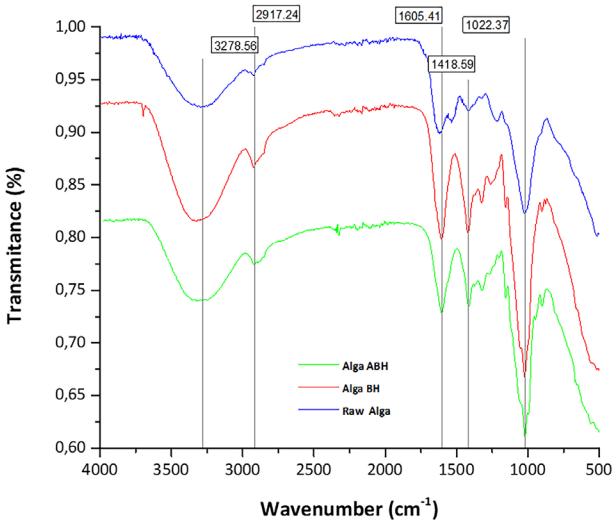

Figure 1. Infrared spectra and identification of the most important wavelengths of the fibers without hydrolysis and after hydrolysis (ABH: acid-base hydrolysis, BH: alkaline hydrolysis, raw alga: without treatment)

Table 3. Results were obtained from the crystallinity index for each of the fibers analyzed

Sample	I_{002}	I_{am}	CrI
Wages ST	22.49	14.26	36.60%
Algae HB	22.82	12.15	46.76%
Algae HAB	27.51	14.36	47.80%

when contrasting the three samples. The increase in the IC with the first treatment occurs because the NaOH after a certain concentration can penetrate the cellulose network to separate the carbohydrates in the amorphous regions (Kljun et al., 2011). The fibers after acid hydrolysis have the highest CrI value since acetic acid has been used to help remove the amorphous part of the fibers, which has been shown in previous investigations using 6.0% acetic acid in the cellulose from African palm rachis (García et al., 2020, 2022; Mesén and Mora, 2021). It is important to highlight that crystallinity levels are not reached as a consequence of the dilution of the reagents and the conditions of the hydrolysis process; however, this level of crystallinity can be used in future research on hydrogels. Figure 2 shows the micrographs obtained after size reduction using high-power ultrasound. This figure shows the hydrolysis. In the said figure, when the transmission electron microscope images are observed, it is noted that the fibers, in both cases, reach a nanometric size. After alkaline hydrolysis, the fibers reached sizes ranging from 135 nm to 190 nm and after acid hydrolysis, fiber sizes are 108 nm and 163 nm.

The size of the fibers is important since they are directly related to the concentration necessary to obtain a three-dimensional gel conformation. When nanocrystals are used, the concentration of nanocellulose must not be less than 10% to achieve gelation, while using nanofibers a gel with a concentration of < 1% is even achieved (De France et al., 2017). Figure 3 shows the drying curves corresponding to the hydrogels with borax at different mass percentages.

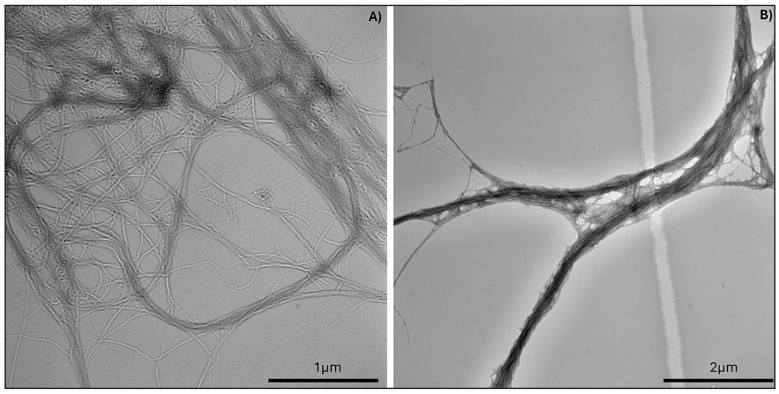

Figure 2. Samples of nanocellulose reduced in size with high-power ultrasonic equipment seen using a transmission electron microscope A) alkaline hydrolysis, B) acid hydrolysis

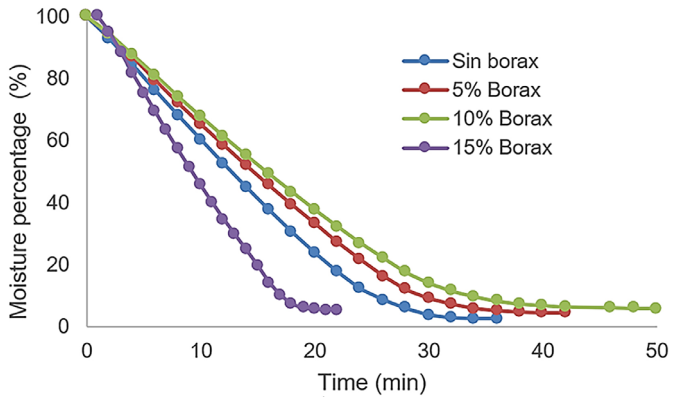

Figure 3. Drying curves of the hydrogels with different concentrations of borax

It is appreciated how the presence of this solid in the hydrogel decreases the ability to release moisture. However, borax favors the release of water at low humidity percentages after exceeding 10% of the mass ratio, and said capacity is diminished as the concentration of such compound increases. This behavior is because at these points the humidity that initially contains the borax ($Na_2B_4O_7 \cdot 10\ H_2O$) is also expelled, which drives out the water found in the pores (Liu et al., 2020). Therefore, it is recommended to use low concentrations of borax in the hydrogel in case you want to maintain said release capacity (Thombare et al., 2017).

Due to these results, the decision was made to prepare the hydrogel with 10% borax, which was later used as a crosslinking agent, and other nutrients was added. With such a strategy, the speed of removal of these nutrients is reduced so that their release is more gradual and uniform. Based on Figure 4, the response of the hydrogel to different concentrations of borax and with the incorporation of the different nutrients used can be analyzed. When looking at the figures, it can be seen how the hydrogel releases nutrients more slowly with 10% borax. This behavior is functional to carry out a correct dosage of nutrients during the germination stage, since if the dosage is very slow, germination is affected and on the other hand, if it is too much, the effect on germination is counterproductive (Kristó et al., 2023). The behavior shown in the hydrogel with 15% borax is the average speed of the study, probably as a consequence of the moisture release mechanism, which could be beneficial in environments with low humidity (Pedroza-Sandoval et al., 2015). However, it was decided to use hydrogel with 10% borax due to its speed of nutrient release. In any case, this last hydrogel also presented a very slow-release rate of potassium dihydrogen phosphate, thus ensuring that the material behaves more uniformly with most nutrients (Fig. 5).

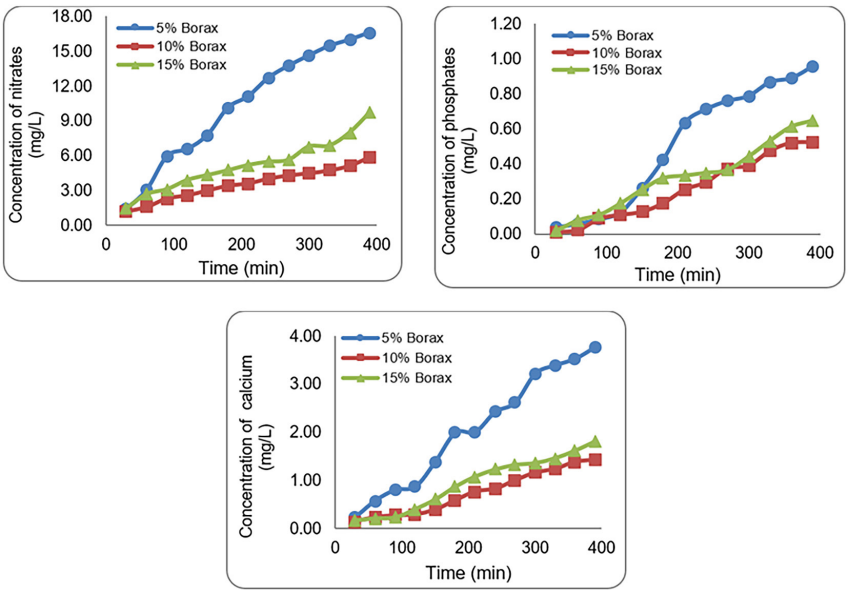

Figure 4. Nutrient release curves for nanocellulose hydrogels with different concentrations of borax

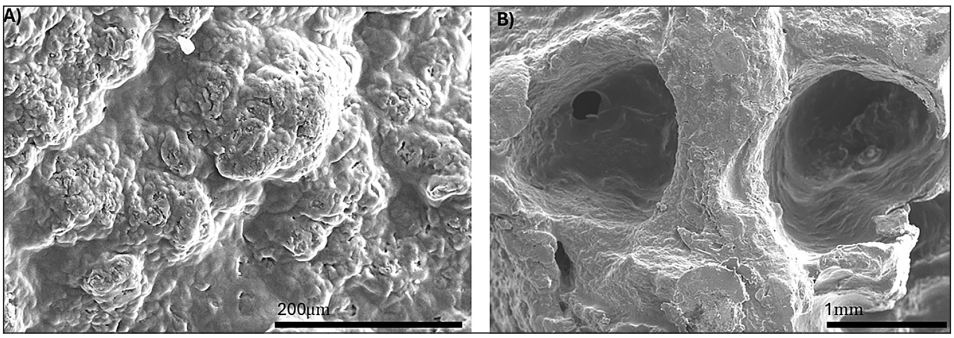

Figure 5. Micrographs made using a scanning electron microscope on the hydrogel a) surface of hydrogel, b) cross-sectional area of hydrogel

From the initial concentration value, it was obtained that the release of nitrogen was 100% for the hydrogels with all borax concentrations, however, for the case of phosphorus and calcium the results are shown in Table 4. It can be observed that the nutrient with the greatest difficulty to be released was phosphorus, however, Follmer et al. (2021) showed that phosphorus, although it influences seed germination, has less effect compared to the other nutrients studied here.

The results of the morphology of the hydrogel were performed by scanning electron microscopy, and the rough surface was observed, however, some internal pores generated by the hydrogel structure were shown on the inside. Figure 6 shows the data referring to the amount of germinated seeds for each of the nutrients and their combinations.

As can be seen, the nutrients with the greatest success of germinated seeds in the case of beans were HSNutri, H-N, and control, while the H-F and H-N/F treatments did not obtain any germinated seeds. In the case of flaxseed, the hydrogels with the lowest number of germinated seeds were the same as in the case of beans, and the one with the highest number of germinated seeds was H-N. This behavior may be due to the excess phosphorus that the hydrogel possessed, in previous investigations, it is mentioned that the maximum dose for 2 weeks is 15 mg/L, if we take as a projection point the result of Table 4 for the biopolymer with 10% of borax, in 12 days more

Table 4. Percentage of nutrient release for each nutrient and different borax concentrations

Nutritious	Borax concentration (%)	Initial concentration (mg/L)	Concentration released at 7 days (mg/L)
Nitrogen	5	100	100
	10	100	100
	15	100	100
Phosphorus	5	100	45.17
	10	100	19.09
	15	100	23.12
Calcium	5	100	100
	10	100	39.22
	15	100	52.40

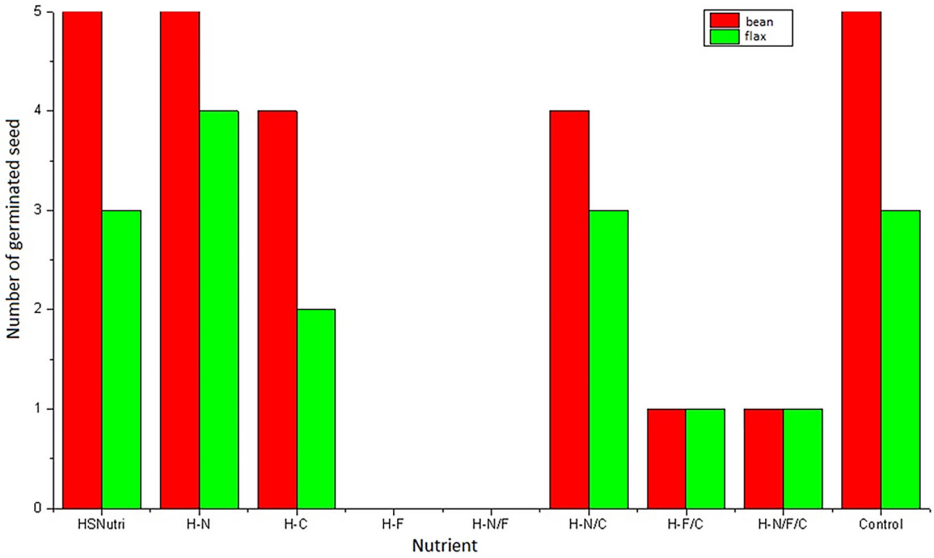

Figure 6. The number of germinated seeds according to the treatment used (HSNutri: hydrogel without nutrients; H-N: hydrogel with nitrogen; H-C: hydrogel with calcium; H-F: hydrogel with phosphorus; H-N/F: hydrogel with nitrogen and phosphorus; H-N/C: hydrogel with nitrogen and calcium; H-F/C: Hydrogel with phosphorus and calcium; H-N/F/C: hydrogel with nitrogen, phosphorus, and calcium; Control: sample without hydrogel) where red bars representing the beans seed and green bars the flax germinated seeds

than 19.09 mg/L would have been dosed; concentration that already exceeds the ideal amount and that, in addition, causes negative results for the growth process (Hernández et al., 2016). Figure 7 shows that the method that favored the initial growth of the plants (greater average stem size) was the H-N method. This result was expected since nitrogen is considered a primary macronutrient (Marschner and Rengel, 2012), in addition, uniformity in the data is shown and, as a consequence, a low deviation. In Figure 8, it may be that the method associated with the largest stem sizes was the H-N but in this case, the deviation is very high. This last detail indicates that there was no uniformity in the response of the plants associated with the different samples and that the results varied greatly among them. Before starting with the statistical analysis of the data, a two-way analysis of variance (ANOVA) was performed to determine if there was any effect of any of the factors studied on the observed results, obtaining a value of p = 0.1057 for the effect of the nutrient used at a value of $p = 2.410 \times 10^{-10}$ to the type of seed.

Therefore, it can be observed that the nutrient used did not present an inference in the general data of stem size, but the type of seed did have an effect. This is logical since, being two different plant species, it was natural to expect large differences in the growth of plants of different species. However, this analysis does not allow

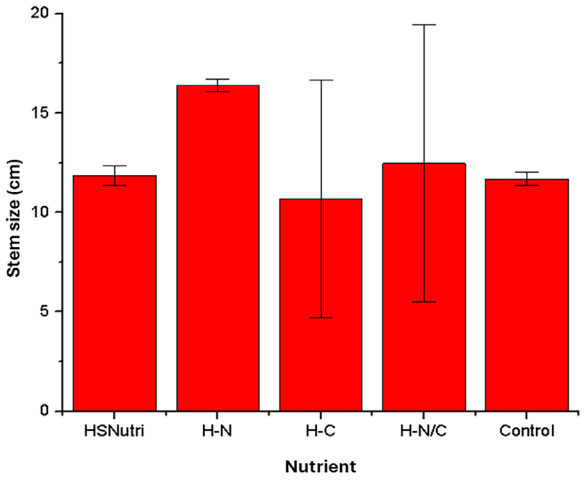

Figure 7. Average stem size for beans according to the treatment applied (HSNutri: hydrogel without nutrients; H-N: Hydrogel with nitrogen; H-C: hydrogel with calcium; H-N/C: hydrogel with nitrogen and calcium; Control: sample without hydrogel) calcium; H-N/C: hydrogel with nitrogen and calcium; Control: sample without hydrogel)

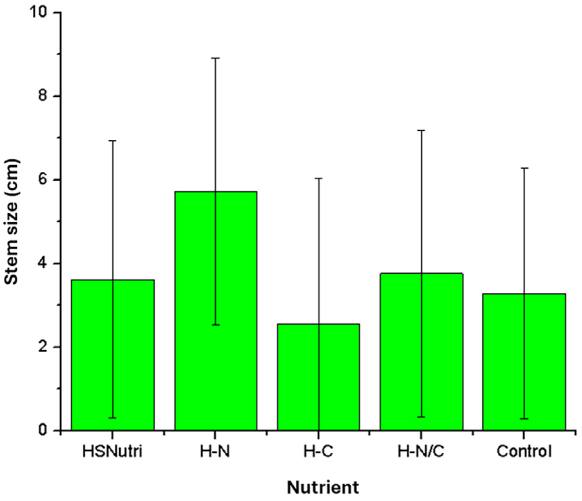

Figure 8. Average stem size for flaxseed according to the treatment applied (HSNutri: hydrogel without nutrients; H-N: hydrogel with nitrogen; H-C: hydrogel with calcium; H-N/C: hydrogel with nitrogen and calcium; Control: sample without hydrogel

an evaluation of the effect of the type of nutrient independently for each type of plant. Therefore.

The statistical analysis of stem sizes, the Shapiro-Wilks normality test was performed as a first step, and after this the Kruskal-Wallis non-parametric analysis was carried out to determine if there are significant differences between the means of each treatment.

As can be seen in the previous results, none of the stem growth data sets associated with each plant species presented normal values. This can be affirmed since both p values in the said test are less than 0.05, the value of α selected for said test. Once this was demonstrated, a non-parametric test was selected that helped us to assess whether there were significant differences in stem size according to the nutrition method used during germination.

The Kruskal-Wallis test established the null hypothesis that the medians of the treatments are not different, while the alternative hypothesis stated that there was at least one nutrition treatment with a different median from the rest. In the case of bean seeds, a p-value less than the critical value (0.05) was obtained, so statistically speaking we can affirm that the null hypothesis is rejected and the alternative hypothesis is accepted. This suggests that there is at least one treatment with a lower or higher median compared to the others. For flaxseeds, the opposite was the case. the resulting p-value in the Kruskall-Wallis test is greater than 0.05, so the null hypothesis is

Table 5. Mann-Whitney test for each treatment applied to bean seeds. Statistically significant values (p less than 0.05) are shown in colored cells

Mann–Whitney test					
	HSNutri	H-N	H-C	H-N/C	Control
HSNutri	x	0.01219	0.1437	0.1437	0.6761
H-N	0.01219	x	0.01219	0.01219	0.01219
H-C	0.1437	0.01219	x	0.1161	0.1437
H-N/C	0.1437	0.01219	0.1161	x	0.1437
Control	0.6761	0.01219	0.1437	0.1437	x

accepted and it can be statistically confirmed that the treatments uniformly affect stem size.

Table 5 shows the results of the Mann-Whitney test for each of the treatments that germinated with the bean seed. The pink color of the cells denotes the interactions with a significant difference between them. This is known since these boxes have numerical values less than 0.05. In the case of flaxseed, this step was not performed since it had previously been shown that there were no statistically significant differences between the nutrition methods.

CONCLUSIONS

It was shown that the results indicated the removal of lignin and the obtaining of nanofibers through both hydrolysis routes using high-power ultrasonic. When using the transmission electron microscope, it was observed that the nanofibers obtained by basic means are dimensionally larger, but they are still within the nanometric range and that the difference in the crystallinity index between both hydrolysis routes is 1.04%. Therefore, the production of nanofibers with basic hydrolysis is viable and has the potential to lower production costs.

As could be observed in the nutrient release curves, evidence was accumulated showing the effectiveness of hydrogels from nanocellulose as a medium for nutritional exchange with culture systems. At the same time, it is observed that the moisture lost, and the release of nutrients are related to the percentage of cross-linking agent used, which is why it is presumed that the amount of borax agent directly affects water retention and nutrient release.

The nutrient with the greatest influence on germination results was nitrogen. This result was expected because nitrogen is the most important nutrient for seed development. In contrast, the nutrient that obtained the worst results was phosphorus and this result may be related to its concentration in the hydrogel. It is very possible that the phosphorus concentration has exceeded the adequate amounts for the evaluated seeds and that this effect has been observed in the results obtained for germination speed and stem size.

Acknowledgements

The authors are thankful to the Unit of Forest Resources (REFORESTA) the Engineering Research Institute (INII), and University of Costa Rica´s Caribbean Headquarters for the financial support.

REFERENCES

1. Ai, N., Jiang, Y., Omar, S., Wang, J., Xia, L., Ren, J. 2022. Rapid Measurement of Cellulose, Hemicellulose, and Lignin Content in Sargassum horneri by Near-Infrared Spectroscopy and Characteristic Variables Selection Methods. Molecules, 27(2), 335. https://doi.org/10.3390/molecules27020335
2. Akhter, J., Mahmood, K., Malik, K.A., Mardan, A., Ahmad, M., Iqbal, M.M. 2004. Effects of hydrogel amendment on water storage of sandy loam and loam soils and seedling growth of barley, wheat, and chickpea. Plant, Soil and Environment, 50(10), 463–469. https://doi.org/10.17221/4059-pse
3. Alzate-Arbeláez, A.F., Dorta, E., López-Alarcón, C., Cortés, F.B., Rojano, B.A. 2019. Immobilization of Andean berry (*Vaccinium meridionale*) polyphenols on nanocellulose isolated from banana residues: A natural food additive with antioxidant properties. Food Chemistry, 294, 503–517. https://doi.org/10.1016/j.foodchem.2019.05.085
4. Chávez-Guerrero, L., Toxqui-Teran, A., Pérez-Camacho, O. 2022. One-pot isolation of nanocellulose using pelagic Sargassum spp. from the Caribbean coastline. Journal of Applied Phycology, 34(1), 637–645. https://doi.org/10.1007/

s10811-021-02643-5

5. De France, K.J., Hoare, T., Cranston, E.D. 2017. Review of Hydrogels and Aerogels Containing Nanocellulose. Chemistry of Materials, 29(11), 4609–4631. https://doi.org/10.1021/acs.chemmater.7b00531
6. Deepa, B., Abraham, E., Cordeiro, N., Mozetic, M., Mathew, A.P., Oksman, K., Faria, M., Thomas, S., Pothan, L.A. 2015. Utilization of various lignocellulosic biomass for the production of nanocellulose: a comparative study. Cellulose, 22(2), 1075–1090. https://doi.org/10.1007/s10570-015-0554-x
7. Follmer, C.M., Hummes, A.P., Lângaro, N.C., Petry, C., Moterle, D.F., Bortoluzzi, E.C. 2021. Nutrient availability and pH level affect germination traits and seedling development of Conyza canadensis. Scientific Reports, 11(1), 15607. https://doi.org/10.1038/s41598-021-95164-7
8. Franks, J.S., Johnson, D.R., Ko, D.S. 2016. Pelagic sargassum in the tropical North Atlantic. Gulf and Caribbean Research, 27(1). https://doi.org/10.18785/gcr.2701.08
9. Gower, J., King, S. 2019. Seaweed, seaweed everywhere. In Science 364(6448), 27. American Association for the Advancement of Science. https://doi.org/10.1126/science.aay0989
10. Hassan, N.S., Badri, K.H. 2014. Lignin recovery from alkaline hydrolysis and glycerolysis of oil palm fiber, 433–438. https://doi.org/10.1063/1.4895236
11. Hernández, G., Toscano, V., Méndez, N., Gómez, L., Mullings, M. 2016. Effect of phosphorus concentration on its assimilation in three common beans (*Phaseolus vulgaris* L.) genotypes. Mesoamerican Agronomy, 7(1), 80. https://doi.org/10.15517/am.v7i1.24794
12. Honorato-Salazar, J.A., Colotl-Hernández, G., Apolinar-Hidalgo, F., Aburto, J. 2016. Main chemical components of the wood of Ceiba pentandra, Hevea brasiliensis, and Ochroma pyramidale. Wood and Forests, 21(2). https://doi.org/10.21829/myb.2015.212450
13. Hospodarova, V., Singovszka, E., Stevulova, N. 2018. Characterization of cellulosic fibers by FTIR spectroscopy for their further implementation to building materials. American Journal of Analytical Chemistry, 9(06), 303. https://doi.org/10.4236/ajac.2018.96023
14. Jirón-García, E.G., Rodríguez Mora, K., Bernal, C. 2020. Cellulose nanofiber production from banana rachis. International Journal of Engineering Science and Computing, 10(2), 24683–24689.
15. Jirón-García, E.G., Rodríguez-Mora, K., Bernal-Samaniego, C. 2022. Obtaining nanocellulose from African palm rachis and sugarcane bagasse. Journal Technology On the Move, 35(2), 167–1 https://doi.org/10.18845/tm.v35i3.5609
16. Jirón-García, E.G., Rodríguez-Mora, K.M. 2022. Functionalization of palm rachis nanocellulose as adsorbent of metal cations from water. InterSedes. https://doi.org/10.15517/isucr.v23i48.49746
17. Jones, C.S., Mayfield, S.P. 2012. Algae biofuels: versatility for the future of bioenergy. Current Opinion in Biotechnology, 23(3), 346–351. https://doi.org/10.1016/j.copbio.2011.10.013
18. Kljun, A., Benians, T.A.S., Goubet, F., Meulewaeter, F., Knox, J.P., Blackburn, R.S. 2011. Comparative analysis of crystallinity changes in cellulose I polymers using ATR-FTIR, X-ray diffraction, and carbohydrate-binding module probes. Biomacromolecules, 12(11), 4121–4126. https://doi.org/10.1021/bm201176m
19. Kristó, I., Vályi-Nagy, M., Rácz, A., Irmes, K., Szentpéteri, L., Jolánkai, M., Kovács, G.P., Fodor, M.Á., Ujj, A., Valentinyi, K.V., Tar, M. 2023. Effects of nutrient supply and seed size on germination parameters and yield in the next crop year of winter wheat (*Triticum aestivum* L.). Agriculture, 13(2), 419. https://doi.org/10.3390/agriculture13020419
20. Kubo, S., Kadla, J.F. 2005. Hydrogen bonding in lignin: A fourier transform infrared model compound study. Biomacromolecules, 6(5), 2815–2821. https://doi.org/10.1021/bm050288q
21. Liu, C., Lei, F., Li, P., Jiang, J., Wang, K. 2020. Borax crosslinked fenugreek galactomannan hydrogel as a potential water-retaining agent in agriculture. Carbohydrate Polymers, 236. 116100. https://doi.org/10.1016/j.carbpol.2020.116100
22. Liu, S., Wu, Q., Sun, X., Yue, Y., Tubana, B., Yang, R., Cheng, H.N. 2021. Novel alginate-cellulose nanofiber-poly (vinyl alcohol) hydrogels for carrying and delivering nitrogen, phosphorus, and potassium chemicals. International Journal of Biological Macromolecules, 172, 330–340. https://doi.org/10.1016/j.ijbiomac.2021.01.063
23. Lu, T., Lu, Y., Hu, L., Jiao, J., Zhang, M., Liu, Y. 2019. Uncertainty in the optical remote estimation of the biomass of Ulva proliferates macroalgae using MODIS imagery in the Yellow Sea. Optics Express, 27(13), 18620. https://doi.org/10.1364/oe.27.018620
24. Marinho-Soriano, E., Fonseca, P.C., Carneiro, M.A.A., Moreira, W.S.C. 2006. Seasonal variation in the chemical composition of two tropical seaweeds. Bioresource Technology, 97(18), 2402–2406. https://doi.org/10.1016/j.biortech.2005.10.014
25. Marschner, P., Rengel, Z. 2012. Chapter 12 - Nutrient Availability in Soils. In P. Marschner (Ed.), Marschner's Mineral Nutrition of Higher Plants (Third Edition) 315–330. Academic Press. https://doi.org/https://doi.org/10.1016/B978-0-12-384905-2.00012-1
26. Mattio, L., Payril, C.E. 2011. 90 Years of Sargassuni Taxonomy, Facing the Advent of DNA Phylogenies.

77, 31–70. https://doi.org/10.100

27. Maurer, A.S., de Neef, E., Stapleton, S. 2015. Sargassum accumulation may spell trouble for nesting sea turtles. Frontiers in Ecology and the Environment, 13(7), 394–395. https://doi.org/10.1890/1540-9295-13.7.394
28. Nagappan, H., Pee, P.P., Kee, S.H.Y., Ow, J.T., Yan, S.W., Chew, L.Y., Kong, K.W. 2017. Malaysian brown seaweeds Sargassum siliquosum and Sargassum polycystum: Low density lipoprotein (LDL) oxidation, angiotensin converting enzyme (ACE), α-amylase, and α-glucosidase inhibition activities. Food Research International, 99, 950–958. https://doi.org/10.1016/j.foodres.2017.01.023
29. Patel, J.P., Parsania, P.H. 2018. Characterization, testing, and reinforcing materials of biodegradable composites. In Biodegradable and Biocompatible Polymer Composites, 55–79. Elsevier. https://doi.org/10.1016/B978-0-08-100970-3.00003-1
30. Pavia, D.L., Lampman, G.M., Kriz, G.S., Vyvyan, J.R. 2009. Introduction to spectroscopy. Brooks/Cole, Cengage Learning.
31. Pazderů, K., Koudela, M. 2013. Influence of hydrogel on germination of lettuce and onion seed at different moisture levels. Journal of the Mendelian University of Agriculture and Forestry in Brunnen, 61(6), 1817–1818. https://doi.org/10.11118/actaun201361061817
32. Pedroza-Sandoval, A., Yáñez-Chávez, L.G., Sánchez-Cohen, I., Samaniego-Gaxiola, J.A. 2015. Effect of hydrogel and vermicomposta on corn production. Mexican Phytotechnics Magazine, 38(4), 375. https://doi.org/10.35196/rfm.2015.4.375
33. Picado White, P. 2022, March. They confirm the arrival of two species of sargassum on the coasts of the southern Costa Rican Caribbean. News University of Costa Rica. https://www.ucr.ac.cr/noticias/2022/03/22/confirman-la-llegada-de-dos-especies-de-sargazo-a-las-costas-del-caribe-costarricense.html
34. Ramírez, I., Niño, G., Boada Eslava, L., Baron, A. 2007. Evaluation of hydrogels for agroforestry applications. Engineering and Research, 27, 35–44.
35. Ray, D., Sain, S. 2017. Plant fiber reinforcements. In D. Ray, Biocomposites for High-Performance Applications 1–21. Woodhead Publishing. https://doi.org/https://doi.org/10.1016/B978-0-08-100793-8.00001-6
36. Resiere, D., Valentino, R., Nevière, R., Banydeen, R., Gueye, P., Florentin, J., Cabié, A., Lebrun, T., Mégarbane, B., Guerrier, G., Mehdaoui, H. 2018. Sargassum seaweed on Caribbean islands: an international public health concern. The Lancet, 392(10165), 2691. https://doi.org/10.1016/S0140-6736(18)32777-6
37. Rivera Fernández, R.D., Mesías Gallo, F. 2018. Hydrogel water absorption for agricultural use and its wetting of three types of soil. FCA UNCuyo Magazine, 50(2), 15–21.
38. Rudzinski, W.E., Dave, A.M., Vaishnav, U.H., Kumbar, S.G., Kulkarni, A.R., Aminabhavi, T.M. 2002. Hydrogels as controlled release devices in agriculture. Designed Monomers and Polymers, 5(1), 39–65. https://doi.org/10.1163/156855502760151580
39. Salem, D.M.S.A., Ismail, M.M. 2022. Characterization of cellulose and cellulose nanofibers isolated from various seaweed species. Egyptian Journal of Aquatic Research, 48(4), 307–313. https://doi.org/10.1016/j.ejar.2021.11.001
40. Schiener, P., Black, K.D., Stanley, M.S., Green, D.H. 2014. The seasonal variation in the chemical composition of the kelp species Laminaria digitata, Laminaria hyperborea, Saccharina latissima, and Alaria esculenta. Journal of Applied Phycology, 27(1), 363–373. https://doi.org/10.1007/s10811-014-0327-1
41. Schwanninger, M., Rodrigues, J.C., Pereira, H., Hinterstoisser, B. 2004. Effects of short-time vibratory ball milling on the shape of FT-IR spectra of wood and cellulose. Vibrational Spectroscopy, 36(1), 23–40. https://doi.org/10.1016/j.vibspec.2004.02.003
42. Segal, L., Creely, J.J., Martin, A.E., Conrad, C.M. 1959. An empirical method for estimating the degree of crystallinity of native cellulose using the X-Ray diffractometer. Textile Research Journal, 29(10), 786–794. https://doi.org/10.1177/004051755902901003
43. Sills, D.L., Gossett, J.M. 2012. Using FTIR to predict saccharification from enzymatic hydrolysis of alkali-pretreated biomasses. Biotechnology and Bioengineering, 109(2), 353–362. https://doi.org/10.1002/bit.23314
44. Sun, J.X., Sun, X.F., Zhao, H., Sun, R.C. 2004. Isolation and characterization of cellulose from sugarcane bagasse. Polymer Degradation and Stability, 84(2), 331–339. https://doi.org/10.1016/j.polymdegradstab.2004.02.008
45. Sun, R., Sun, X.F., Tomkinson, J., Wang., N. 2000. Fractional isolation and physicochemical characterization of alkali-soluble lignins from fast-growing poplar wood. Polymer, 41(23), 8409–8417.
46. Supramaniam, J., Adnan, R., Mohd Kaus, N.H., Bushra, R. 2018. Magnetic nanocellulose alginate hydrogel beads as a potential drug delivery system. International Journal of Biological Macromolecules, 118, 640–648. https://doi.org/10.1016/j.ijbiomac.2018.06.043
47. Svobodová, H., Nonappa, Lahtinen, M., Wimmer, Z., Kolehmainen, E. 2012. A steroid-based gelator of A(LS)2 type: tuning gel properties by metal coordination. Soft Matter, 8(30), 7840. https://doi.org/10.1039/c2sm25259g
48. Tamayo, J.P., Del Rosario, E.J. 2014. Chemical analysis and utilization of sargassum sp. as

substrate for ethanol production. Iranica Journal of Energy and Environment, 5(2), 202–208. https://doi.org/10.5829/idosi.ijee.2014.05.02.12

49. Thombare, N., Jha, U., Mishra, S., Siddiqui, M.Z. 2017. Borax cross-linked guar gum hydrogels as potential adsorbents for water purification. Carbohydrate Polymers, 168, 274–281. https://doi.org/10.1016/j.carbpol.2017.03.086
50. Van Tussenbroek, B.I. 2016. Afluencia masiva de sargazo pelágico a la costa del Caribe mexicano (2014–2015). Caribe Mexicano. 353–365.
51. Vargas Mesén, J., Rodríguez Mora, K. 2021. Nanocellulose functionalization from pineapple stubble and African palm rachis. Scientific, 25(2), 1–19. https://doi.org/10.46842/ipn.cien.v25n2a08
52. Vargas Mesén, J., Rodríguez Mora, K., Jirón García, E., Bernal Samaniego, C. 2023. Producción de nanocelulosa a partir de rastrojo de piña y raquis de palma africana. UNED Research Journal, 15(2), e4593. https://doi.org/10.22458/urj.v15i2.4593
53. Wang, M., Hu, C., Barnes, B.B., Mitchum, G., Lapointe, B., Montoya, J.P. 2019. The great Atlantic Sargassum belt. Science, 365(6448), 83–87. https://doi.org/10.1126/science.aaw7912
54. Wang, M., Hu, C., Cannizzaro, J., English, D., Han, X., Naar, D., Lapointe, B., Brewton, R., Hernandez, F. 2018. Remote sensing of sargassum biomass, nutrients, and pigments. Geophysical Research Letters, 45(22), 12, 359–12, 367. https://doi.org/10.1029/2018GL078858
55. Wang, Y., Shaghaleh, H., Hamoud, Y.A., Zhang, S., Li, P., Xu, X., Liu, H. 2021. Synthesis of a pH-responsive nano-cellulose/sodium alginate/MOFs hydrogel and its application in the regulation of water and N-fertilizer. International Journal of Biological Macromolecules, 187, 262–271. https://doi.org/10.1016/j.ijbiomac.2021.07.154
56. Yende, S., Harle, U., Chaugule, B. 2014. Therapeutic potential and health benefits of Sargassum-species. In Pharmacognosy Reviews, 8(15), 1–7. https://doi.org/10.4103/0973-7847.125514
57. Zhang, H., Yang, M., Luan, Q., Tang, H., Huang, F., Xiang, X., Yang, C., Bao, Y. 2017. Cellulose anionic hydrogels based on cellulose nanofibers as natural stimulants for seed germination and seedling growth. In J. Agric. Food Chem., Journal of Agricultural and Food Chemistry65 (19), 3785-3791. https://doi.org/10.1021/acs.jafc.6b05815